Multicarrier Signal Detection and Parameter Estimation in Frequency-Selective Rayleigh Fading Channels

Toshiaki Kuroda, *Member, IEEE,* and Tadashi Matsumoto, *Senior Member, IEEE*

***Abstract*—A new joint signal detection and channel parameter estimation scheme is proposed for multiple subcarrier signaling with pilot symbol-assisted modulation (PSAM) schemes. The proposed scheme estimates a pair of parameters associated with the generation process of the fading frequency selectivity, which is common to all the subcarriers. This parameter estimation can effectively extract information regarding the fading frequency selectivity through the pilot symbols received not only by the subcarrier of interest, but by other ones as well. The fading complex envelope with each subcarrier is derived from the estimates of the parameter pair. With the proposed scheme, performances are evaluated through simulations and are compared with performances of a subcarrier-by-subcarrier detection scheme.**

***Index Terms*—Channel estimation, digital cellular system, frequency selectivity, multicarrier signal detection, pilot symbol-assisted modulation (PSAM).**

I. Introduction

In MULTIPLE subcarrier signaling, the entire bandwidth is divided into several *consecutive* subbands, in each of which the subcarrier frequency centered at the center of the subband is modulated by a relatively low-speed digital signal. If the symbol rate of each subcarrier is f_s and there are M subcarriers, the total symbol rate is Mf_s. This total symbol rate may require an entire bandwidth larger than or equivalent to the channel coherence bandwidth. However, each subcarriers' bandwidth is small enough to prevent the received signal from being damaged by intersymbol interference (ISI). Hence, multiple subcarrier signaling is effective in reducing the effects of fading frequency selectivity encountered in mobile communications channels. The need for channel equalizers, which might be required for a single carrier signaling scheme with the same (total) symbol rate (Mf_s), is eliminated.

Recently, pilot symbol-assisted modulation (PSAM) has been proposed [1]–[4] for mobile communication applications, where the fading complex envelope is estimated using pilot symbols periodically embedded in the information symbol sequence to be transmitted. For coherent detection, the complex conjugate of the fading envelope estimate is multiplied by the received signal sample. References [2] and [3] use interpolation techniques for the fading estimation and apply it to the multilevel quadrature amplitude modulation (QAM) signal transmission over Rayleigh fading channels. References [1] and [4] combine the PSAM signal detection with decoding of trellis codes. Recently, [5] analyzes the performance limit of the pilot-assisted coherent signal detection, where a Wiener filter is used to minimize the variance of the estimation error within the class of linear filters.

When PSAM is used in subcarrier signaling, unlike the case of single carrier, information about the fading complex envelope can be more frequently extracted by locating the pilot symbols at different timings for *some* of the subcarriers. Even then, the frequency of the pilot transmission remains constant for each of the subcarriers. This suggests the use of pilot symbols for more precise fading estimation than the single carriers case, while keeping the overall spectrum efficiency (=*per-subcarrier information symbol rate*/f_s) constant. With multiple subcarrier signaling, each of the subcarriers suffers from almost frequency-flat fading because $\tau f_s \ll 1$, where τ is the channel delay spread. The fading complex envelopes with the M subcarriers are different from each other, but correlate closely. Therefore, if fading estimation for coherent detection takes place subcarrier-by-subcarrier, this scheme utilizes neither the frequent pilot symbol reception nor the fading correlation among the subcarriers.

The motivation of this work is to develop a new joint signal detection and channel parameter estimation scheme for the coherent detection of multiple subcarrier PSAM signals. The proposed scheme *does not* estimate the fading complex envelope with *each* subcarrier in a straightforward manner, but *estimates* a pair of parameters associated with the generation process of the fading frequency selectivity, which is common to the M subcarriers. The fading complex envelope with *each* subcarrier can be derived from the estimates of the parameter pair. Hence, this process makes effective use of the pilot symbols received by different subcarriers (not necessarily the one of interest). The proposed scheme is not an equalizer for ISI cancellation because if an equalizer is used in the multiple subcarrier system, the benefits of $\tau \ll T$ will be missing.

The proposed scheme uses two types of Kalman algorithm for parameter estimation. A standard recursive least-square (RLS) algorithm is first used to obtain estimates of the parameter pair for known symbols such as pilot symbols. Assuming that the parameter pair at symbol timing n can be expressed as a function $\mathbf{f}(n)$ of n, a decision-directed

Manuscript received December 15, 1995; revised October 10, 1996. This work was supported by the NEXTEL/NTT Project.

T. Kuroda is with Nippon Telegraph and Telephone Corporation (NTT), Japan.

T. Matsumoto is with NTT Mobile Communications Network, Inc., Japan.

Publisher Item Identifier S 0018-9545(97)05111-6.

Kalman algorithm with $\mathbf{f}(n+1)-\mathbf{f}(n)$ as a control force is then used to obtain the estimates of the parameter pair for information symbols. Interpolation or curve-fitting schemes may be used to determine $\mathbf{f}(n)$ from the estimates for the known symbols.

This paper is organized as follows. Section II shows the system model used in this paper, describes mathematical expressions for the model, and defines the goal of this work as a joint detection and parameter estimation problem. Section III derives algorithm for the estimation of the parameter pair for pilot and information symbols. Section IV shows the results of computer simulations for the performance evaluations with the proposed scheme. Four-subcarrier pilot symbol-assisted 16QAM (4-PSAM/16QAM) is used as a modulation scheme for the simulations. The performance of the proposed scheme is compared with that of the coherent detection based on subcarrier-by-subcarrier fading estimation.

II. System Model

The entire bandwidth is divided into M *consecutive* subbands having center frequencies of

$$f_k = (k-1)\Delta f \tag{1}$$

where $1 \le k \le M$ and Δf is the channel separation required to prevent adjacent subcarriers from interfering with the subband signals. It is assumed throughout this paper that with appropriate choices of Δf and a rolloff filter the interference from the adjacent subcarriers can be ignored.[1] The kth subcarrier has a center frequency of f_k. Each subcarrier is modulated by a relatively low-speed digital signal. It is assumed that a multilevel phase-amplitude modulation scheme is used such as phase-shift keying (PSK) or QAM and that the same modulation scheme is used for all the M subcarriers.

1) Transmitter: The kth subcarrier is modulated by the symbol sequence $s_k(n)$ to be transmitted, where $n \in (-\infty, +\infty)$ is the symbol timing index. $s_k(n)$ $(= I + jQ$, where I and Q are the in-phase and quadrature components, respectively) takes one of the signal points defined as a modulation alphabet. It is assumed that the M subcarriers' symbol timings are synchronized with each other. The symbol sequence is segmented into frames with length of N_f (MN_f symbols in a frame in total). Fig. 1(a) shows an example of the frame format. The information symbol sequence is headed by a unique word sequence with length of N_u (MN_u symbols in total). The pilot symbols are periodically embedded in the information symbol sequence. The pilot symbols are located at different timings for *some* of the subcarriers (this is referred to as "offset pilot location" for convenience) so that receivers can extract information about the fading complex envelope more frequently than for the single carrier's cases.

Fig. 1(b) shows a block diagram of the transmitter in the equivalent complex baseband domain. The symbol sequence $s_k(n)$ is filtered by a rolloff filter for spectrum shaping. It is assumed that the overall transfer function of the Nyquist rolloff filter is shared equally by transmitter and receiver. Hence, the modulating signal $Z_{mk}(t)$ of the kth subcarrier is the output wave form of the root Nyquist rolloff filter. The composite signal $Z_t(t)$ comprised of the M modulated subcarriers can then be expressed as

$$Z_t(t) = \sum_{k=1}^{M} Z_{mk}(t) e^{j\omega_k t} \tag{2}$$

where $\omega_k = 2\pi f_k$. This complex composite signal is upconverted and transmitted.

2) Channel: It is assumed that the fading frequency selectivity is due to an N-path propagation scenario [6]. The equivalent baseband transfer function $h(t)$ of the N-path Rayleigh fading channel can be expressed as

$$h(t) = \sum_{l=1}^{N} Z_{fl}(t)\delta(t-\tau_l) \tag{3}$$

where $Z_{fl}(t)$ and τ_l are, respectively, the fading complex envelope and the delay with the lth propagation path, and $\delta(\cdot)$ is the delta function. Without loss of generality, $\tau_1 = 0$ is assumed. Because of the multiple subcarrier signaling, the channel delay spread $\tau = \mathrm{Max}(\tau_i)$ is assumed to be small enough compared with the symbol duration T $(=1/f_s)$.

3) Receiver: Fig. 1(c) shows a block diagram of the receiver. For the kth subcarrier, the output $Z_{rk}(t)$ of the root Nyquist receiver filter becomes

$$Z_{rk}(t) = \sum_{l=1}^{N} Z_{fl}(t) Z_k(t-\tau_l) e^{-j\omega_k\tau_l} + Z_{nk}(t) \tag{4}$$

where $Z_k(t)$ is the overall response of the Nyquist rolloff filter to the input symbol sequence $s_k(n)$ given by

$$Z_k(t) = \sum_{n=-\infty}^{\infty} s_k(n) h_r(t-nT) \tag{5}$$

with

$$h_r(t) = \frac{\sin(\pi t/T)}{\pi t/T} \cdot \frac{\cos(\alpha\pi t/T)}{1-(2\alpha t/T)^2} \tag{6}$$

being the overall impulse response of the filter and α being the rolloff factor, and $Z_{nk}(t)$ is the additive white Gaussian noise component on the kth subcarrier.

The receiver does not use an equalizer for the ISI cancellation. The receiver filter output is sampled at each symbol timing nT. Ignoring the ISI components in (5), because of $\tau \ll T$, the filter output sample can be approximated as

$$z_{rk}(n) \approx s_k(n) \sum_{l=1}^{N} z_{fl}(n) h_r(-\tau_l) e^{-j\omega_k\tau_l} + z_{nk}(n) \tag{7}$$

where $z_{fl}(n) = Z_{fl}(nT)$, $z_{rk}(n) = Z_{rk}(nT)$, and $z_{nk}(n) = Z_{nk}(nT)$. It is found from (7) that $z_{Fk}(n)$ defined by

$$z_{Fk}(n) = \sum_{l=1}^{N} z_{fl}(n) h_r(-\tau_l) e^{-j\omega_k\tau_l} \tag{8}$$

is the (frequency-flat) fading complex envelope the kth subcarrier is suffering from. Note that $z_{fl}(n)$ and $z_{nk}(n)$ are

[1] The class of the system discussed in this paper includes an orthogonal frequency-division multiplexing scheme [7].

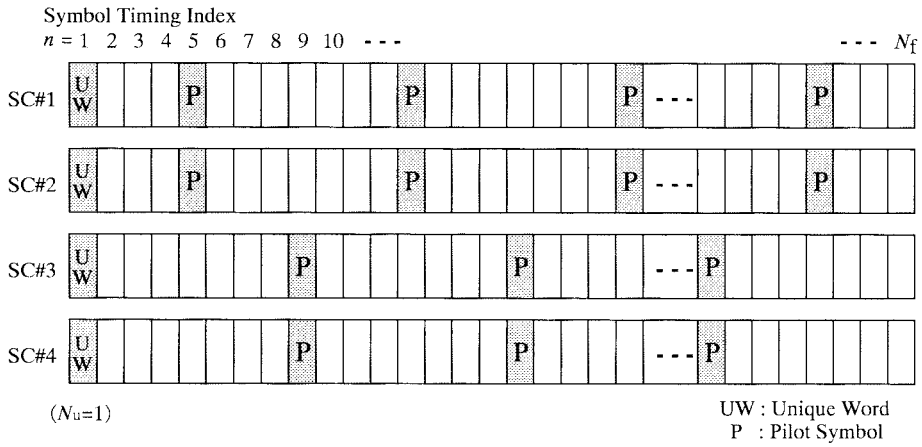

(a)

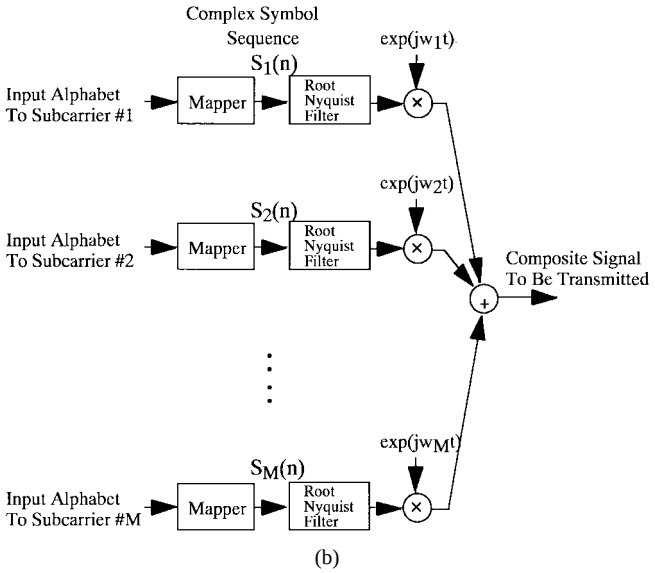

(b)

Fig. 1. (a) Example of frame format for multiple subcarrier PSAM. (b) Block diagram of transmitter.

zero-mean complex Gaussian processes with variances of $\langle |z_{fl}(n)|^2 \rangle = \sigma_{fl}^2$, and $\langle |z_{nk}(n)|^2 \rangle = \sigma_{nk}^2$, respectively. If the average signal power $\langle |s_k(n)|^2 \rangle = 1$, the average received signal-to-noise power ratio (SNR) Γ_k for the kth subcarrier is defined as $\Gamma_k = \sum_{l=1}^{N} \sigma_{fl}^2/\sigma_{nk}^2$.

Coherent detection requires an estimate $\hat{z}_{Fk}(n)$ of $z_{Fk}(n)$. $\hat{z}_{Fk}^*(n)/|\hat{z}_{Fk}(n)|^2$ is multiplied by $z_{rk}(n)$, where $*$ denotes the complex conjugate, and a symbol closest to $z_{rk}(n)\hat{z}_{Fk}^*(n)/|\hat{z}_{Fk}(n)|^2$ is then selected from among the modulation alphabets and output as a decision result. Hence, the objective of joint signal detection and parameter estimation for the multiple subcarrier PSAM is to provide coherent detectors with accurate estimates $\hat{z}_{Fk}(n)$'s of $z_{Fk}(n)$'s for each subcarrier using known symbols, such as the unique word and pilot symbols, as well as the previous decision results for the information symbols. For subcarrier-by-subcarrier detection, the fading estimation schemes for single carrier PSAM [1]–[4] can be used. However, this does not take into account the generation process of the fading frequency selectivity expressed in (3), which is common to the M subcarriers, nor does it exploit the benefit of the offset pilot location.

III. Algorithm

A. Proposed Scheme

The fact that $\tau \ll T$ is used again. Ignoring higher order terms of τ in (8), $z_{Fk}(n)$ can be approximated as

$$z_{Fk}(n) \approx x_1(n) + j\omega_k x_2(n) \tag{9}$$

where

$$x_1(n) = z_{f1}(n) + \sum_{l=2}^{N} z_{fl}(n) h_r(-\tau_l) \tag{10}$$

and

$$x_2(n) = -\sum_{l=2}^{N} \tau_l z_{fl}(n) h_r(-\tau_l). \tag{11}$$

The parameter pair of $x_1(n)$ and $x_2(n)$ is associated with the generation process of the fading frequency selectivity and is independent of k. If the estimates $\hat{x}_1(n)$ and $\hat{x}_2(n)$ of the parameter pair can be obtained, the estimate $\hat{x}_{Fk}(n)$ of the fading complex envelope $z_{Fk}(n)$ for the kth subcarrier can

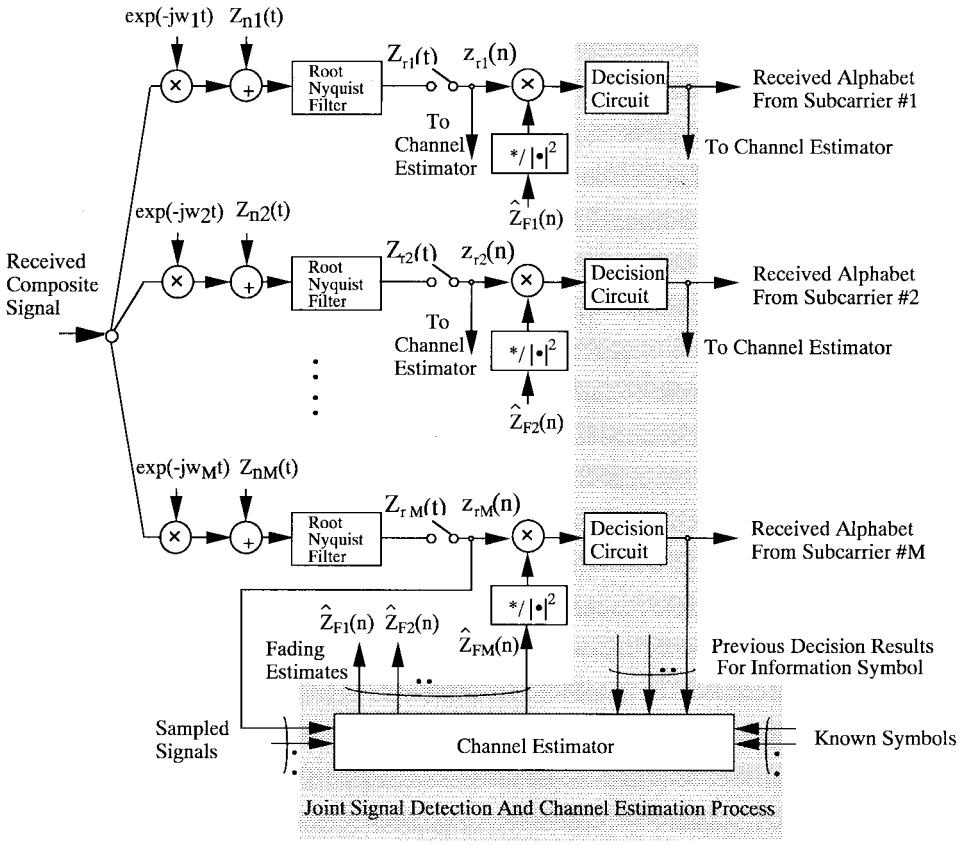

(c)

Fig. 1. (*Continued.*) (c) Block diagram of receiver.

also be obtained by using (9). Hence, the proposed scheme aims to estimate the vector $\mathbf{x}(n) = [x_1(n) \quad x_2(n)]^t$ instead of $z_{Fk}(n)$ itself.

The proposed scheme is comprised of two stages. A standard RLS algorithm is first used for the known symbols, and a decision-directed Kalman algorithm is then used for the information symbols.

1) Parameter Estimation for Known Symbols: The ordering of signal processing for the known symbols is from small to large n (but not contiguous) corresponding to the pilot symbol timings. Let the ordering for signal processing be reindexed by contiguous i. Fig. 2(a) shows, for example, the ordering of signal processing for the frame format of Fig. 1(a). The state-space representation of the channel

$$\mathbf{x}(i+1) = \mathbf{x}(i) + I_2 w(i) \tag{12}$$

$$z_{rk}(i) = \mathbf{c}(i)\mathbf{x}(i) + z_{nk}(i) \tag{13}$$

is then used for the parameter estimation, where

$$\mathbf{c}(i) = [\tilde{s}_k(i) \quad -j\omega_k \tilde{s}_k(i)] \tag{14}$$

is the observation vector with $\tilde{s}_k(i)$ being the known symbol at a certain pilot timing corresponding to the signal processing index i. $w(i)$ is the process noise, I_L is the $L \times L$ unit matrix, and k is the index of the subcarrier on which the known symbols are transmitted.

Because the unique word and pilot symbols are known, $s_k(i)$'s are known. Hence, a standard RLS algorithm [8] can be used for this state-space representation to obtain $\mathbf{x}(i)$'s estimate $\hat{\mathbf{x}}(i)$ as

$$\hat{\mathbf{x}}(i) = \hat{\mathbf{x}}(i-1) + P(i-1)\mathbf{c}(i)^H \cdot \frac{[z_{rk}(i) - \mathbf{c}(i)\hat{\mathbf{x}}(i-1)]}{\mathbf{c}(i)P(i-1)\mathbf{c}(i)^H + \lambda} \tag{15}$$

$$P(i) = \frac{\sigma_n^2}{\lambda}\left[P(i-1) - \frac{P(i-1)\mathbf{c}(i)^H\mathbf{c}(i)P(i-1)}{\mathbf{c}(i)P(i-1)\mathbf{c}(i)^H + \lambda}\right] \tag{16}$$

with $\hat{\mathbf{x}}(0) = \mathbf{0}$ and $P(0) = \rho I_2$, where $P(i) = \langle[\hat{\mathbf{x}}(i) - \mathbf{x}(i)][\hat{\mathbf{x}}(i) - \mathbf{x}(i)]^H\rangle$ with H denoting the transposed complex conjugate of a matrix, ρ is some positive large number, and λ is a constant given by

$$\lambda = \frac{\sigma_{nk}^2}{1 + \sigma_w^2}. \tag{17}$$

Note that the noise variance σ_{nk}^2 is usually unknown. $\sigma_{nk}^2 = 1$ may be used that does not significantly affect the performance. Note further that σ_w^2 is usually unknown. With $\sigma_{nk}^2 = 1$, the forgetting factor $\lambda = 1/(1 + \sigma_w^2)$ is used to control the speed of the algorithm convergence instead of σ_w^2, where $0 < \lambda \leq 1$.

2) Parameter Estimation for Information Symbols: When the recursion of (15) and (16) reaches the last pilot symbol in the frame, we have $\mathbf{x}(i)$'s estimates, $\hat{\mathbf{x}}(i)$'s, for every known symbol. $\hat{\mathbf{x}}(i)$'s are then used to obtain estimates of the parameter pair for the information symbols that are unknown to the receiver. The proposed estimation scheme described below is decision directed. As shown in Fig. 2(b), the symbol

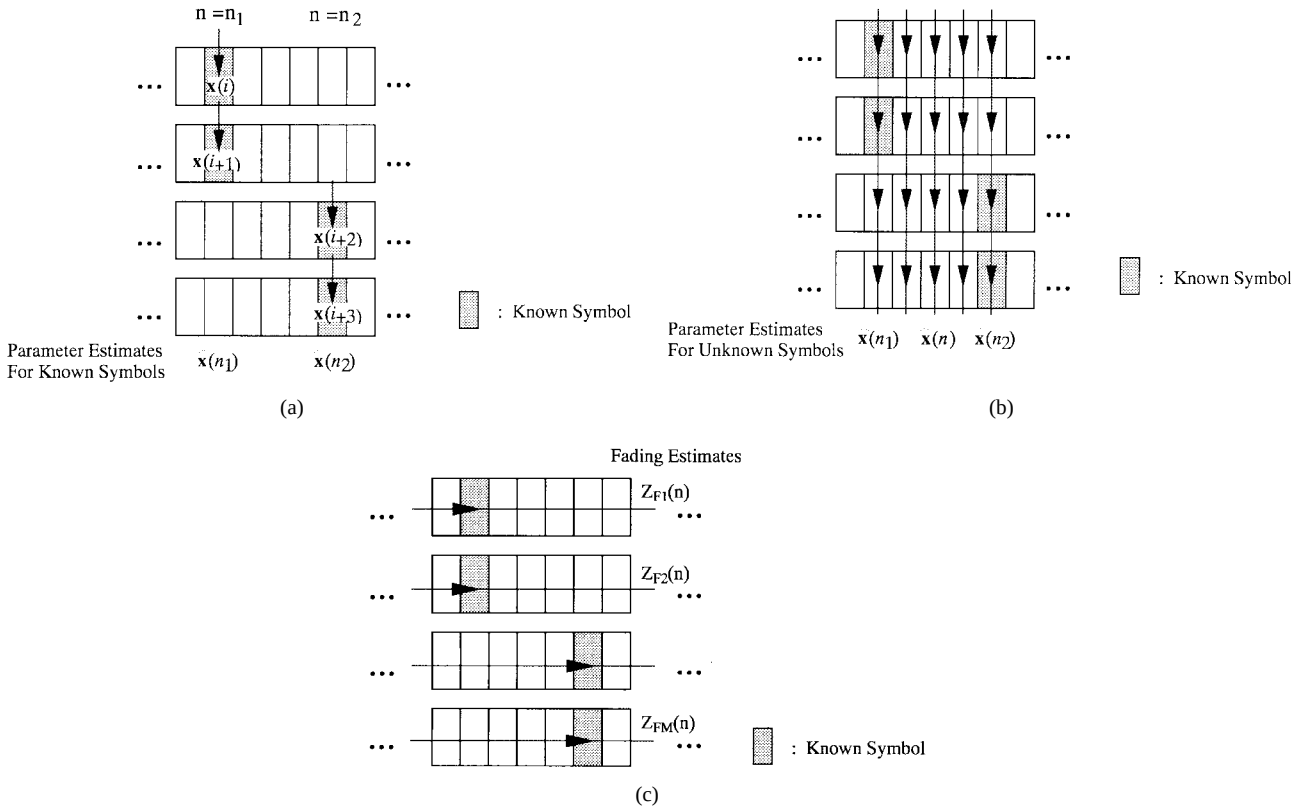

Fig. 2. (a) Ordering of signal processing for known symbols. (b) Ordering of signal processing for unknown symbols. (c) Ordering of signal processing for subcarrier-by-subcarrier estimation.

timing index n is used for the ordering of signal processing. Let us assume that during a time interval $n_1 \le n \le n_2$, the values of the parameter pair $\mathbf{x}(n) = [x_1(n) \quad x_2(n)]^t$ vary as a function $\mathbf{f}(n)$ of n. Interpolation [2], [3] or curve-fitting schemes using the estimates of several known symbols on both sides as indexed in time may be used to determine $\mathbf{f}(n)$. From $\mathbf{x}(n) = \mathbf{f}(n)$, $\mathbf{x}(n+1) = \mathbf{x}(n) + \mathbf{g}(n)$, where $\mathbf{g}(n) = \mathbf{f}(n+1) - \mathbf{f}(n)$ is the control force that forcibly drives the parameter vector. For example, if an order P polynomial of n is used for $\mathbf{f}(n)$ as

$$\mathbf{f}(n) = \sum_{p=0}^{P} \mathbf{a}_p n^p$$

$\mathbf{g}(n)$ then becomes

$$\mathbf{g}(n) = \sum_{p=1}^{P} \sum_{q=0}^{p-1} \mathbf{a}_p \binom{p}{q} n^q$$

where $\mathbf{a}_p = (a_{p1}, a_{p2})^t$ with $0 \le p \le P$.

Hence, for $n_1 \le n \le n_2$ the state-space representation of the channel becomes

$$\mathbf{x}(n+1) = \mathbf{x}(n) + \mathbf{g}(n) + I_2 w(n) \tag{18}$$

$$\mathbf{z}_r(n) = C(n)\mathbf{x}(n) + I_M z_n(n) \tag{19}$$

where

$$\mathbf{z}_r(n) = [z_{r1}(n) \quad z_{r2}(n) \quad \cdots \quad z_{rM}(n)]^t \tag{20}$$

and

$$C(n) = \begin{bmatrix} s_1(n) & -j\omega_1 s_1(n) \\ s_2(n) & -j\omega_2 s_2(n) \\ \vdots & \vdots \\ s_M(n) & -j\omega_M s_M(n) \end{bmatrix}. \tag{21}$$

For this state-space representation with $\mathbf{g}(n)$ as a control force, we have the following recursive algorithm:

$$\begin{aligned} \hat{\mathbf{x}}(n) = \hat{\mathbf{x}}(n-1) &+ \mathbf{g}(n-1) + P(n-1)C(n)^H \\ &\cdot [C(n)P(n-1)C(n)^H + \lambda I_M]^{-1} \\ &\cdot [z_{rk}(n) - C(n)\{\hat{\mathbf{x}}(n-1) + \mathbf{g}(n-1)\}] \end{aligned} \tag{22}$$

$$\begin{aligned} P(n) = \frac{\sigma_n^2}{\lambda}[&P(n-1) - P(n-1)C(n)^H \\ &\times [C(n)P(n-1)C(n)^H + \lambda I_M]^{-1} C(n)P(n-1)] \end{aligned} \tag{23}$$

with $\hat{\mathbf{x}}(n_1) = \mathbf{f}(n_1)$ and $P(n_1) = \rho I_2$.

Unlike the estimation process for known symbols, the information symbols $s_k(n)$'s are unknown when the recursion reaches the index n. Hence, decisions on the unknown symbols on the M subcarriers have to be made prior to the recursion of (22) and (23). To do this, $\hat{\mathbf{x}}(n)$ is estimated from $\hat{\mathbf{x}}(n-1)$ as

$$\hat{\mathbf{x}}(n) = \hat{\mathbf{x}}(n-1) + \mathbf{g}(n-1). \tag{24}$$

The estimate of the fading complex envelope for the kth subcarrier, required for the coherent detection at symbol timing n, can then be obtained from (9). Decisions on $s_k(n)$'s can then be made. The process described above is repeated for

other intervals (n_1, n_2)'s for the detection of other information symbols between the known unique word and/or pilot symbols.

Note that if $n_2 - n_1$ is relatively small, it may be reasonable that for $n \in (n_1, n_2)$ the parameter vector $\mathbf{x}(n)$ varies as a linear function of n as $\mathbf{x}(n) = \mathbf{f}(n) = \mathbf{a}_1 n + \mathbf{a}_0$, where $\mathbf{a}_1 = (a_{11}, a_{12})^t$ and $\mathbf{a}_0 = (a_{01}, a_{02})^t$. In this case, the control force $\mathbf{g}(n) = \mathbf{f}(n+1) - \mathbf{f}(n) = \mathbf{a}_1$. If n_1 and n_2 are the symbol timings for the known symbols, a reasonable choice for $\mathbf{a}_1$ is

$$\mathbf{a}_1 = \frac{\hat{\mathbf{x}}(n_2) - \hat{\mathbf{x}}(n_1)}{n_2 - n_1} \tag{25}$$

for $n_1 \le n \le n_2$. If there is more than one known symbol in one symbol timing, the estimate vector having the highest index i among them may be used.

B. Subcarrier-by-Subcarrier Estimation

Subcarrier-by-subcarrier estimation aims to estimate directly the fading complex envelope $z_{Fk}(n)$ itself. As shown in Fig. 2(c), this process takes place for each subcarrier *independently* of other carriers. The estimates $\hat{z}_{Fk}(n)$'s of $z_{Fk}(n)$'s for the information symbols can be obtained in the same way as the estimates $\hat{\mathbf{x}}(n)$'s of the parameter vector $\mathbf{x}(n)$'s were obtained. The two-stage estimation process described above can be applied to state-space representations of $z_{Fk}(n)$'s for the known and the information symbols. This is fairly straightforward and hence will not be described in detail.

IV. Simulation Results

This section shows the results of computer simulations conducted for the performance evaluations with the proposed scheme. Four-PSAM/16QAM is used as a modulation scheme for the simulations (there are four subcarriers having a PSAM format). The symbol-error rate (SER) performances with the proposed scheme are compared with the subcarrier-by-subcarrier estimation and detection scheme. The frame format described in Fig. 1(a) is used. The frame is 60 symbols long $(N_f = 60)$, and the unique word is one symbol long $(N_u = 1)$. Because there are four subcarriers, one frame is comprised of 240 16QAM symbols. The pilot symbols are transmitted every eight symbols per subcarrier, but their positions are different among the subcarriers. At the receiver, the pilot symbols are received every four symbol timings.

It is assumed that the rolloff factor of the Nyquist filter $\alpha = 0.5$. The channel separation between the subcarriers $\Delta f / f_s$ normalized by the per-subcarrier symbol rate f_s is 1.125 so that with $\alpha = 0.5$ the interference components from the adjacent subcarriers can be ignored. An equal-power two-path propagation model $(N = 2)$ was assumed. It was also assumed that for all the M subcarriers, $\Gamma_k = \Gamma$. $\mathbf{f}(n) = \mathbf{a}_1 n + \mathbf{a}_0$ was used as the control force, where $\mathbf{a}_1$ was determined using (25).

The behavior of the estimated fading complex envelopes $\hat{z}_{Fk}(n)$'s for the four subcarriers is demonstrated in Fig. 3(a) for the delay spread τ/T and the maximum Doppler frequency

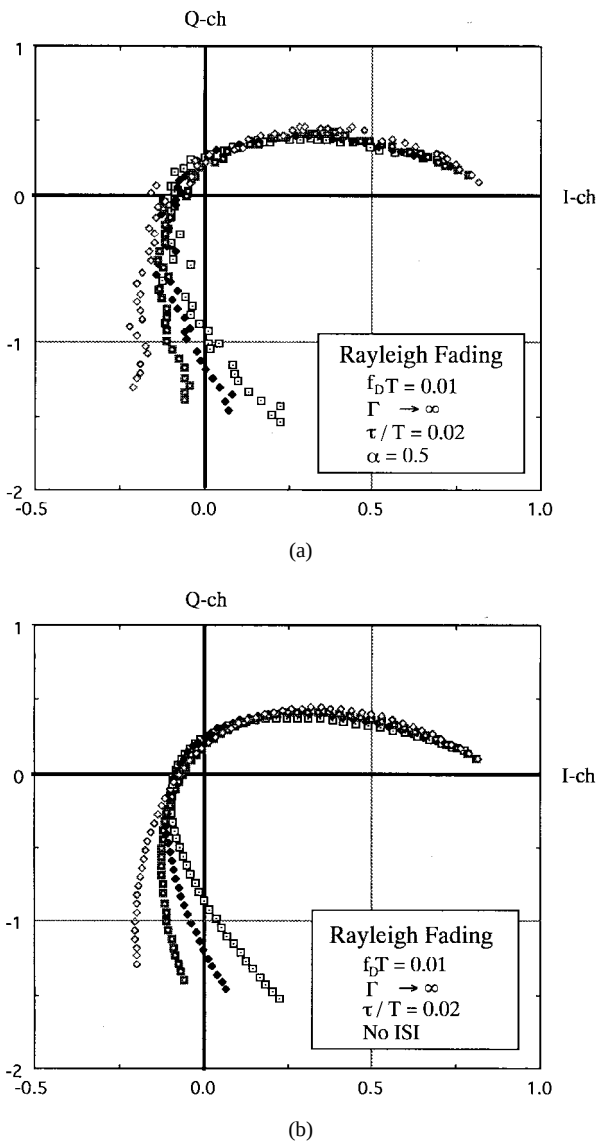

Fig. 3. (a) Behavior of estimated fading complex envelopes with four subcarriers. (b) Behavior of actual fading complex envelopes with four subcarriers.

f_DT, both normalized by symbol duration T of, respectively, 0.02 and 0.01, and the per-carrier average received SNR of $\Gamma \rightarrow \infty$. Fig. 3(b) shows the behavior of their corresponding actual $z_{Fk}(n)$'s. It is found that $\hat{z}_{Fk}(n)$'s track $z_{Fk}(n)$'s relatively well, however, they fluctuate around the trajectory of $z_{Fk}(n)$'s. This is mainly because the ISI components from the adjacent symbols ignored in the proposed parameter estimation scheme [see (7)] in fact perturb the algorithm convergence.

Fig. 4 shows the SER performances with the proposed scheme and the subcarrier-by-subcarrier detection scheme versus per-carrier average received SNR Γ with f_DT and τ/T as parameters (both normalized by symbol duration T). For both cases of $\tau/T = 0$ and $\tau/T = 0.02$, the proposed scheme achieves better performance than the subcarrier-by-subcarrier scheme. When $\tau/T = 0$, the theoretical average SER for the

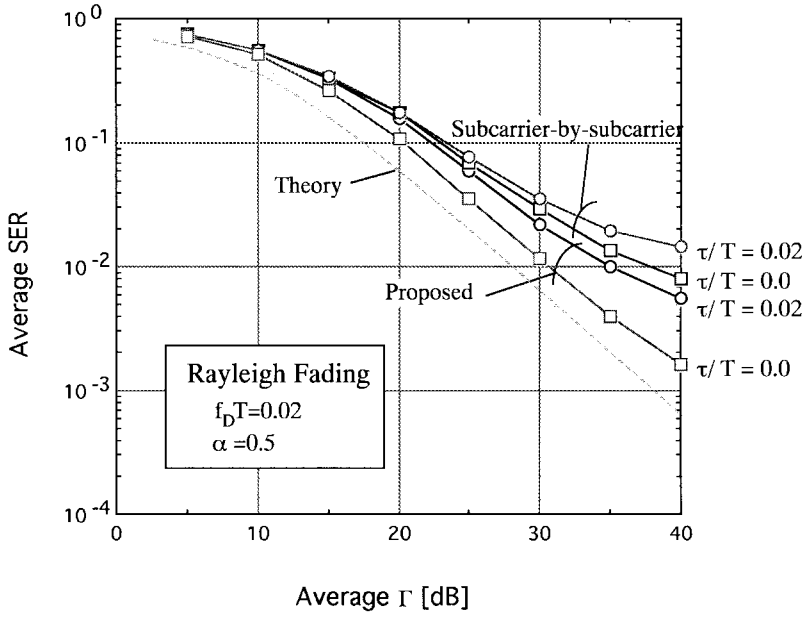

Fig. 4. SER performances versus per-subcarrier average SNR.

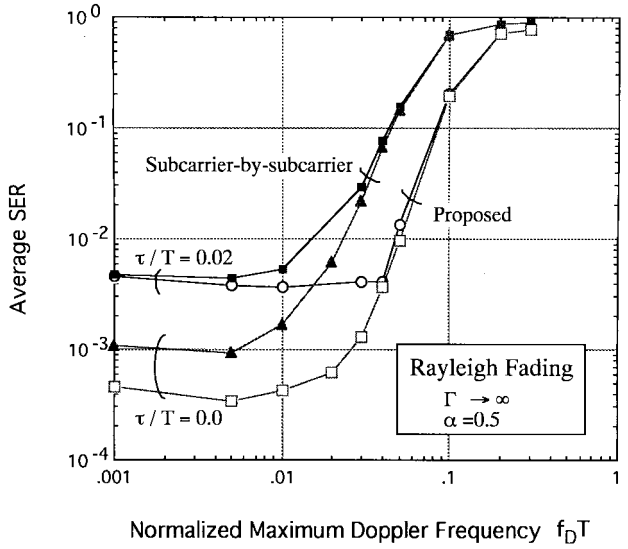

Fig. 5. SER performances versus normalized maximum Doppler frequency.

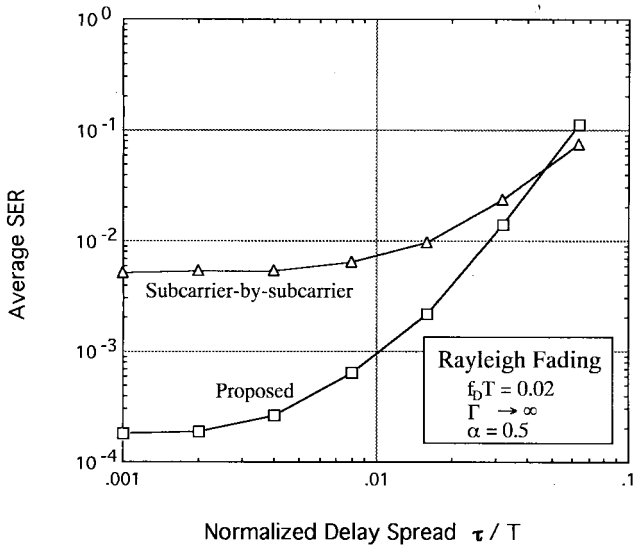

Fig. 6. SER performances versus normalized delay spread.

16QAM coherent detection can be calculated from [9]

$$\text{Average SER} = \int_0^\infty \frac{3}{2}\text{erfc}\left(\sqrt{\frac{\gamma}{10}}\right) \cdot \left[1 - \frac{3}{8}\text{erfc}\left(\sqrt{\frac{\gamma}{10}}\right)\right] \cdot p(\gamma)\, d\gamma \quad (26)$$

where $p(\gamma)$ is the probability density function pdf of the received *instantaneous* SNR γ. Under Rayleigh fading, $p(\gamma) = (1/\Gamma)\exp(-\gamma/\Gamma)$. The theoretical average SER is also plotted in Fig. 4. It is found that with $\tau/T = 0$, the proposed scheme's average SER is roughly 3.0 dB worse than the theoretical one.

Fig. 5 shows for $\Gamma \to \infty$ the SER performances versus f_DT with τ/T as a parameter. It is found that with $\tau/T = 0.02$, the average SER of the proposed scheme is almost identical to that of the subcarrier-by-subcarrier scheme when the normalized maximum Doppler frequency f_DT is relatively small. This is because in a small value range of f_DT, the performances are dominated by the ISI components ignored in both the proposed and subcarrier-by-subcarrier schemes. With $\tau/T = 0$, the SER performances of both the proposed and subcarrier-by-subcarrier schemes also plateau as f_DT becomes smaller, even though there is no ISI. This is because the covariance matrix $P(i)$ or $P(n)$ in the Kalman algorithm tends to be singular when $f_DT \to 0$ and $\Gamma \to \infty$. When f_DT becomes large, the proposed scheme achieves better SER performance than the subcarrier-by-subcarrier scheme for both $\tau/T = 0$ and $\tau/T = 0.02$. This clearly indicates how effective it is to use the knowledge about the channel obtained by other subcarriers' signal detection processes.

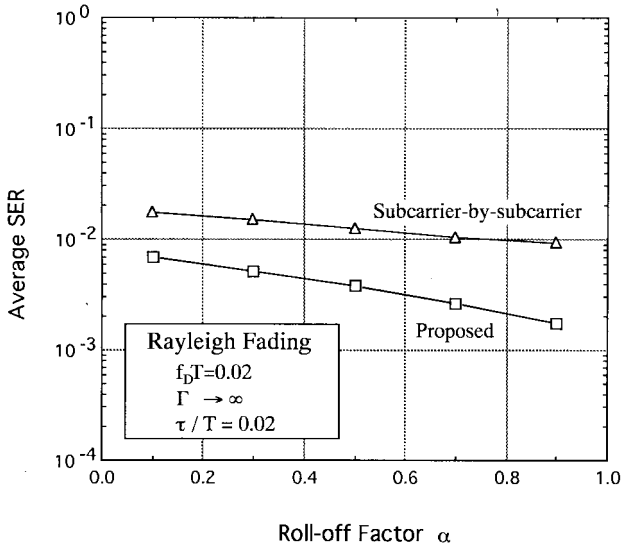

Fig. 7. SER performances versus rolloff factor.

Fig. 6 shows the SER performances versus τ/T for $\Gamma \to \infty$ and $f_DT = 0.02$. The SER performance with the proposed scheme is worse than the performance with the subcarrier-by-subcarrier scheme when $\tau/T > 0.05$. A system design that allows $\tau/T > 0.05$ does not take full advantage of multiple subcarrier signaling. When $\tau/T \leq 0.05$, the proposed scheme achieves smaller SER than the subcarrier-by-subcarrier scheme.

In (7), the ISI components from the adjacent symbols, which is due to the fading frequency selectivity, were ignored because $\tau \ll T$. In fact, the ISI places bit-error rate (BER) floors in the performance curves. The ISI effects depend on the rolloff factor α. Fig. 7 shows the SER performance versus α for $\Gamma \to \infty$, with $\tau/T = 0.02$ and $f_DT = 0.02$. It is found that better performance can be achieved by larger α values. The SER is less sensitive to the α value with the subcarrier-by-subcarrier scheme than with the proposed scheme.

V. Conclusion

In this paper, we have proposed for multiple subcarrier PSAM a new joint detection and channel estimation scheme for mobile communication applications. The proposed scheme makes effective use of $\tau \ll T$, the benefit of which is attributed to multiple subcarrier signaling. In multiple subcarrier signaling, because of $\tau \ll T$, each subcarrier suffers from frequency-flat fading, even though the composite signal comprised of all the subcarrier signals suffers from frequency-selective fading. The proposed scheme does not estimate the fading complex envelope subcarrier-by-subcarrier in a straightforward manner, but estimates a parameter pair associated with the generation process of the fading frequency selectivity. Since this generation process is common to all the subcarriers, locating the pilot symbols at different timings for some (or each) of the subcarriers makes it possible to run the parameter estimation algorithm more frequently for known symbols than the single carrier's case. In fact, this offset pilot location has significantly contributed to the improvements in tracking performance with parameter estimation.

Two types of Kalman algorithm were used for parameter estimation. A standard RLS algorithm is first used to obtain estimates of the parameter pair for known symbols such as pilot symbols. A decision-directed Kalman algorithm with a control force, determined from the results of the RLS algorithm for the known symbols, is then used to obtain estimates of the parameter pair for information symbols.

The performance superiority with the proposed scheme over the subcarrier-by-subcarrier scheme has been demonstrated through computer simulations for 4-subcarrier PSAM/16QAM. It has been shown that even with a relatively high user mobility, which is expressed in terms of the normalized maximum Doppler frequency f_DT, the proposed scheme achieves better performance than the subcarrier-by-subcarrier scheme if the normalized delay spread τ/T is smaller than 0.05. The performance sensitivity to the choice of the control force is to be discussed in near opportunities.

References

[1] M. L. Moher and J. H. Lodge, "TCMP—A modulation and coding strategy for Rician fading channels," *IEEE J. Select. Areas Commun.*, vol. 7, pp. 1347–1355, Dec. 1989.
[2] S. Sampei and T. Sunaga, "Rayleigh fading compensation for 16QAM in land mobile radio communications," *IEEE Trans. Veh. Technol.*, vol. 42, pp. 137–147, May 1993.
[3] T. Sunaga and S. Sampei, "Performance of multi-level QAM with post-detection maximal ratio combining space diversity for digital land-mobile radio communications," *IEEE Trans. Veh. Technol.*, vol. 42, pp. 294–301, Aug. 1993.
[4] A. N. D'Andrea, A. Diglio, and U. Menglai, "Symbol-aided channel estimation with nonselective fading channels," *IEEE Trans. Veh. Technol.*, vol. 44, pp. 41–49, Feb. 1995.
[5] J. K. Cavers, "An analysis of pilot symbol-assisted modulation for Rayleigh fading channels," *IEEE Trans. Veh. Technol.*, vol. 40, pp. 686–693, Nov. 1991.
[6] W. C. Jakes, *Microwave Mobile Communications*. New York: IEEE Press, 1974.
[7] L. J. Cimini, Jr., "Analysis and simulation of a digital mobile channel using orthogonal frequency division multiplexing," *IEEE Trans. Commun.*, vol. COM-33, pp. 665–675, July 1985.
[8] S. Haykin, *Adaptive Filter Theory*. Englewood Cliffs, NJ: Prentice-Hall, 1986.
[9] J. G. Proakis, *Digital Communications*. New York: McGraw-Hill, 1983.

Toshiaki Kuroda (M'95) received the B.S. and M.S. degrees in electrical engineering from Nagoya university, Nagoya-shi, Japan, in 1988 and 1990, respectively.

From 1990 to 1991, he was involved in the development of NTT's microwave radio relay system. From 1991 to 1993, he was dedicated to the algorithm development of a centralized base-station control for NTT's personal handyphone system. In 1994, he surveyed technology trends in wireless local loop systems. From February 1995 to March 1996, he participated in an NTT–NEXTEL joint project as a Technical Advisor. He led the speech quality evaluation of NEXTEL's system. In April 1996, he returned to NTT (Tokai Regional Communications Sector). Since then, he has been surveying recent technical and business trends in telecommunications. Presently, he is an Associate Manager at the Engineering Development Department of NTT Tokai.

Mr. Kuroda is a Member of the Institute of Electronics, Information, and Communication Engineers of Japan.

Tadashi Matsumoto (M'84–SM'95) received the B.S., M.S., and Doctorate degrees in electrical engineering from Keio University, Yokohama-shi, Japan, in 1978, 1980, and 1991, respectively.

He joined Nippon Telegraph and Telephone Corporation (NTT) in April 1980. From April 1980 to May 1987, he researched signal transmission technologies, such as modulation/demodulation schemes, as well as radio link design for mobile communications systems. He participated in the R&D project of NTT's high-capacity mobile communications system, where he was responsible for the development of the base-station transmitter/receiver equipment for the system. From May 1987 to February 1991, he researched error-control strategies, such as forward-error correction (FEC), trellis-coded modulation (TCM), and automatic repeat request (ARQ) in digital mobile radio channels. He developed an efficient new ARQ scheme suitable to the error occurrence in TDMA mobile signal transmission environments. He was involved in the development of a Japanese TDMA digital cellular mobile communications system. He took the leadership for the development of the facsimile and data communications service units for the system. In July 1992, he transferred to NTT Mobile Communications Network, Inc. (NTT DoCoMo). From February 1991 to April 1994, he was responsible for research on code-division multiple-access (CDMA) mobile communications systems. He intensively researched multiuser detection schemes for multipath mobile communications environments. He was also responsible for research on error-control schemes for CDMA mobile communications systems. He concentrated on research of the maximum *a posteriori* probability (MAP) algorithm and its reduced complexity version for decoding of concatenated codes. He took the leadership for the development of error-control equipment for NTT DoCoMo's CDMA mobile communications system. From 1992 to 1994, he served as a part-time Lecturer at Keio University. In April 1994, he moved to NTT America, where he served as a Senior Technical Advisor of the joint project with NTT and NEXTEL Communications. In March 1996, he returned to NTT DoCoMo. Since then, he has been researching time–space signal processing for very high-speed mobile signal transmission. Presently, he is an Executive Research Engineer at NTT DoCoMo.

Dr. Matsumoto is a Member of the Institute of Electronics, Information, and Communication Engineers of Japan.